

A Real-Time Algorithm for Determining the Optimal Paint Gun Orientation in Spray Paint Applications

Pål Johan From, *Member, IEEE*, and Jan Tommy Gravdahl, *Senior Member, IEEE*

Abstract—In this paper, we present a method for increasing the speed at which a standard industrial manipulator can paint a surface. The approach is based on the observation that a small error in the orientation of the end effector does not affect the quality of the paint job. It is far more important to maintain constant velocity throughout the trajectory. We consider the freedom in the end-effector orientation as functional redundancy and represent the restriction on the orientation error as barrier functions or linear matrix inequalities. In doing this, we cast the problem of finding the optimal orientation at every time step into a convex optimization problem that can be solved very efficiently and in real time. We show that the approach allows the end effector to maintain a higher constant velocity throughout the trajectory guaranteeing uniform paint coating and substantially reducing the time needed to paint the object.

Note to Practitioners—This paper is motivated by the observation that uniform paint coating cannot be achieved in steep turns. Even if the manipulator possesses the necessary actuator torques to maintain constant speed for a straight line trajectory the torques needed to maintain constant velocity during turn are far higher. Thus, the operator has to lower the trajectory speed, also in the straight line segments where this would normally not be necessary, or accept a thicker layer of paint in the turns. The method proposed in this paper is to implement a slightly different planning algorithm in turns allowing the paint gun to follow the trajectory with a higher constant velocity. This will allow the paint gun to follow the trajectory, including both straight line segments and turns, with constant velocity and thus achieve uniform paint coating. We show how to choose the desired orientation of the paint gun at every time step and present the explicit expressions for solving and implementing the algorithms.

The approach can also be used for other applications where introducing a freedom in the end-effector orientation improves performance, such as welding and high-pressure water steaming.

Index Terms—Assembly-line manufacturing, convex optimization, functional redundancy, modeling, robotics, spray painting.

I. INTRODUCTION

ONE OF THE most important benefits of introducing industrial manipulators to the assembly line in automotive manufacturing in the 1980s was the removal of all human

Manuscript received December 31, 2008; revised June 23, 2009. Date of publication November 20, 2009; date of current version October 06, 2010. This paper was recommended for publication by Associate Editor M. Nakano and Editor M. Zhou upon evaluation of the reviewers' comments. The authors acknowledge the support of the Norwegian Research Council and the TAIL IO project for their continued funding and support. The TAIL IO Project is an international cooperative research project led by StatoilHydro and an R&D consortium consisting of ABB, IBM, Aker Solutions, and SKF.

The authors are with the Department of Engineering Cybernetics, Norwegian University of Science and Technology, 7491 Trondheim, Norway (e-mail: from@itk.ntnu.no).

Digital Object Identifier 10.1109/TASE.2009.2033567

workers from the spray paint area, relieving them from a toxic working environment. It is crucial for the flow of the automotive assembly line that spray painting is performed both with high quality and in an efficient manner. In this paper, we address the problem of reducing the time needed to paint a surface without compromising the quality of the coating. This is based on the observation that the velocity at which the end effector follows the path is far more important to guarantee uniform paint coating than the orientation of the end effector.

We assume that the tool center point trajectory, i.e., the trajectory at the surface that the paint gun is to follow, is known. Several approaches for finding the optimal path in terms of speed, coverage, and paint waste have been presented in literature. An automatic trajectory planning system is presented by Suh *et al.* [1]. Both the painting mechanics and the robot dynamics are used to find the optimal trajectory with respect to paint uniformity and cycle time given a CAD model. Ramabhadran and Antonio [2], [3] present a computationally efficient formulation of the trajectory tracking problem in spray paint application, while Kim and Sarma [4] find the optimal sweeping paths by minimizing the cycle time subject to actuator speed limits and coating thickness.

Some work has also been done on modeling the paint composition on a surface. Hertling *et al.* [5] present a mathematical model of the paint coating for a tilted gun and Conner *et al.* [6] develop computationally tractable analytic deposition models that allow us to include the paint model, including the orientation with respect to the surface, when considering the paint coating. Smith *et al.* [7] discuss the problem of minimizing the orientation error when following curved surfaces and Atkar *et al.* [8] include the paint model in their framework for optimizing cycle time and coating quality.

In [9], the idea of introducing the paint quality as a constraint and minimize some additional cost function was presented. This opens for the possibility of allowing a small error in the orientation of the end effector in order to increase the velocity of the paint gun, reduce torques and so on. It was shown by From and Gravdahl [10] that by allowing an orientation error, the speed and quality of the job was improved. However, the optimal orientation error was chosen intuitively and the approach presented was not suitable for implementation in an optimization algorithm.

In [11], the problem of friction force limit constraints was transformed into a problem of testing for positive definiteness of a certain matrix. In [12], the same ideas were used to convert the problem of orientation error constraints into a test of positive definiteness of a matrix. For different types of orientation errors, a suitable matrix was found and it was shown that pos-

itive definiteness of this matrix is equivalent to an orientation satisfying the given restrictions.

By transforming the nonlinear orientation constraints into positive definiteness constraints imposed on certain symmetric matrices, we transform the problem of finding the optimal orientation into an optimization problem on the smooth manifold of linearly constrained positive definite matrices. For the special case of positive definite symmetric matrices, the constraints can be written on the form of linear matrix inequalities (LMIs). We also show how to write the constraints as barrier functions and how to solve these. Convex optimization problems involving LMIs or barrier functions have been extensively studied in literature, and reliable and efficient solutions are known (see Boyd *et al.* [13]–[15]).

II. PROBLEM STATEMENT

There are two main factors that play important roles in obtaining uniform paint coating in automotive manufacturing. The first is to move the paint gun with constant velocity throughout the trajectory. This is, in general, an easy task in following straight lines but can be a challenge in turns where high accelerations are required. The second factor is the orientation of the paint gun with respect to the surface, which should be orthogonal. It can be shown that the velocity of the paint gun is far more important than the orientation when it comes to uniform paint coating. A small orientation error ($< 20\%$) in the paint gun does not affect the quality of the coating to the same extent as changes in the velocity. Based on these observations, we represent the orientation not as one frame, but as a constrained continuous set of frames. The problem treated in this paper is then formulated as follows:

Given a maximum allowed orientation error of the paint gun and a trajectory on the surface that the paint gun is to follow with constant velocity and with a fixed distance from the paint gun to the trajectory. Then, the problem is to find the orientation of the paint gun at every point on the trajectory that allows it to follow the trajectory with the highest possible constant velocity.

We note that in this paper, we do not require the orientation to be optimal. The optimal solution to this problem, considering both kinematics and dynamics, is extremely complex. However, we formulate the problem as an optimization problem based on a simple and intuitive cost function and show that the solution to this problem substantially improves performance. In the following, we will denote the solution to this optimization problem the “optimal orientation” although strictly speaking there might exist other orientations that improve performance even further.

We consider a standard industrial manipulator, in our case the ABB IRB-5400 series which is illustrated in Fig. 1. The first three joints are referred to as the main axes, or the main joints. These are the strongest joints and also the ones that require the most torque. While the main axes are mainly used for positioning the paint gun, the last three joints, referred to as the wrist joints, determine the orientation of the paint gun. We fix the inertial reference frame to the base of the manipulator. We also attach a frame to the end effector of the manipulator, in our case the paint gun. This is attached so that the end-effector z

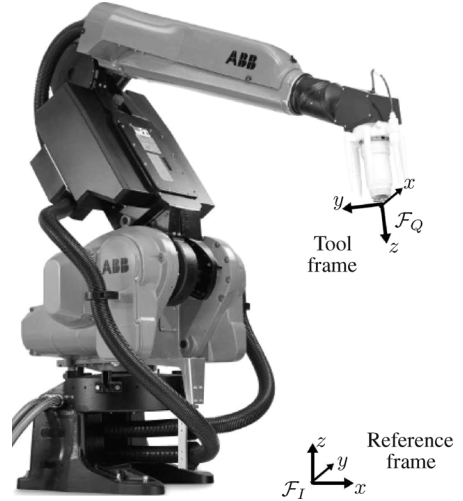


Fig. 1. The ABB IRB spray paint robot with the definitions of the reference and tool frames. Picture courtesy of ABB Robotics.

axis is aligned with the direction of the paint flow. This axis is referred to as the central axis of the end effector.

To find the optimal orientation, we first need to define a set of allowed orientations from which we can choose the optimal one. This set of orientations is defined using the unit quaternion which allows us to rewrite the constraints using very simple expressions. Sections III and IV give a brief background on representing orientations and continuous sets of orientations of rigid bodies. We also show how we can rewrite restrictions on the direction of the central axis as a simple constraint on the unit quaternion. In Section V, we present the theoretical background on how to write constraints on the orientation in a convex optimization setting and in Section VI, we provide the equations needed for implementing the algorithms such that a solution can be found in real time.

In Section VII, we show how we can increase the speed at which the manipulator can paint a given surface without compromising the paint quality. The solution in itself is very simple. It basically allows us to distribute the workload more evenly on the different joints. In our case, we find that for the main joints the actuator torques are very close to the torque limits, while the wrist joints use only a fraction of the torque available. We thus choose the orientations in a way that will make the main joints move less, and thus require less torque. One easy way to do this is to force the position of the wrist towards the center of the surface reducing the length of its trajectory. Keeping in mind that the main joints are mainly used for displacement, this will reduce the required torques of these joints. Section VII also includes several simulations to verify the efficiency of the approach presented.

III. REPRESENTING ROTATIONS

A. The Unit Quaternion

The unit quaternion is well suited for representing orientations or continuous sets of orientations of rigid bodies. A good

introduction to quaternions is found in [16]. Any positive rotation ϕ about a fixed unit vector \mathbf{n} can be represented by the four-tuple

$$Q = \begin{bmatrix} q_0 \\ \mathbf{q} \end{bmatrix} \quad (1)$$

where $q_0 \in \mathbb{R}$ is known as the scalar part and $\mathbf{q} \in \mathbb{R}^3$ as the vector part. $Q(\phi, \mathbf{n})$ is written in terms of ϕ and \mathbf{n} by

$$q_0 = \cos\left(\frac{\phi}{2}\right), \quad \mathbf{q} = \sin\left(\frac{\phi}{2}\right)\mathbf{n}. \quad (2)$$

Q is a quaternion of unit length and denoted a *unit quaternion*. Henceforth, all quaternions have unit length unless otherwise stated. Let $Q_P = [p_0 \ \mathbf{p}^\top]^\top$. The quaternion product of a rotation Q followed by a rotation Q_P is written in vector algebra notations as

$$Q_P * Q = \begin{bmatrix} p_0 q_0 - \mathbf{p} \cdot \mathbf{q} \\ p_0 \mathbf{q} + q_0 \mathbf{p} + \mathbf{p} \times \mathbf{q} \end{bmatrix}. \quad (3)$$

The cross product implies that quaternion multiplication is not commutative, as expected. Let $Q_P = [p_0 \ p_1 \ p_2 \ p_3]^\top$ and $Q = [q_0 \ q_1 \ q_2 \ q_3]^\top$. Then, the quaternion product is written as

$$Q_P * Q = \begin{bmatrix} p_0 q_0 - p_1 q_1 - p_2 q_2 - p_3 q_3 \\ p_0 q_1 + p_1 q_0 + p_2 q_3 - p_3 q_2 \\ p_0 q_2 + p_2 q_0 + p_3 q_1 - p_1 q_3 \\ p_0 q_3 + p_3 q_0 + p_1 q_2 - p_2 q_1 \end{bmatrix}. \quad (4)$$

The quaternion product of two unit quaternions is a unit quaternion. From the definition of the quaternion, we see that the quaternions Q and $-Q$ produce the same rotation. This dual covering allows every rotation to be described twice. In this paper all angles are assumed to be in the interval $[-\pi, \pi]$ so every orientation corresponds to one specific quaternion. It is also assumed that all angles of inverse trigonometric functions are in this interval with the correct sign. For arctan, this is denoted arctan2. The quaternion identity representing the inertial frame is given by $Q_I = [1 \ 0 \ 0 \ 0]^\top$.

A pure quaternion is a quaternion with zero scalar part. Any vector, $\bar{\mathbf{v}} = [x \ y \ z]^\top$ can be represented by a pure quaternion $\mathbf{v} = [0 \ \bar{\mathbf{v}}^\top]^\top$. Finally, the conjugate of a quaternion is defined as $Q^* = [q_0 \ -q_1 \ -q_2 \ -q_3]^\top$.

B. Vector Rotations

Let a vector $\bar{\mathbf{v}}_1$ be represented by the pure quaternion \mathbf{v}_1 . This vector can be rotated ϕ radians around the axis \mathbf{n} by

$$\mathbf{v}_2 = Q * \mathbf{v}_1 * Q^*. \quad (5)$$

Every vector $\bar{\mathbf{v}} \in \mathbb{R}^3$ can be represented by a pure quaternion, hence \mathbf{v} is not necessarily of unit length. The quaternion Q , however, is unitary. This represents the angle and the axis that the vector $\bar{\mathbf{v}}_1$ is rotated about. The resulting vector $\bar{\mathbf{v}}_2$ is then of the same length as $\bar{\mathbf{v}}_1$ if and only if Q is a unit quaternion.

Note that (3) rotates one frame into another frame. By a *frame*, it is meant a coordinate system in \mathbb{R}^3 using Cartesian coordinates. One frame with respect to another frame represents three degrees of freedom and is referred to as *orientation*. The

reference frame is the inertial frame denoted \mathcal{F}_I and the frame that corresponds to the inertial frame by a rotation Q is denoted \mathcal{F}_Q . Equation (5), however, rotates one vector into another vector and represents two degrees of freedom, i.e., a point on a sphere. A unit vector with respect to a unit reference vector is referred to as *direction*. Henceforth, the main concern is with the direction of the central axis, which is assumed to be the body frame z axis of the end effector. We refer to Ha *et al.* [17] for a good reference on vectors and attitudes. The following lemmas will also be used.

Lemma 3.1: (Sylvester's criterion) A matrix P is positive definite if and only if all the leading principal minors are positive. P is positive semi-definite if all the leading principal minors are non-negative.

Lemma 3.2: A block diagonal matrix $P = \text{Blockdiag}(P_1, \dots, P_i, \dots, P_k)$ is symmetric positive definite if and only if each block P_i , $i = 1, \dots, k$ is symmetric positive definite. P is positive semi-definite if each block is positive semi-definite.

IV. QUATERNION VOLUMES

We start by representing a continuous set of orientations defined by a set of constraints in Euler angles and a sequence of rotations. This allows us to find the corresponding constraints on the quaternion entries q_0, q_1, q_2 , and q_3 . We denote this continuous set of quaternions a *quaternion volume*. We then use this intuitive and well defined tool in the next sections to represent these constraints as LMIs or barrier functions.

A. General Definition

A set of frames corresponding to a reference frame by a rotation ϕ about a fixed axis \mathbf{n} can be represented as

$$Q(\phi, \mathbf{n}), \quad \text{for } \phi_{\min} \leq \phi \leq \phi_{\max}. \quad (6)$$

When the rotations are not limited to one axis only, a more general description of all allowed orientations can be represented by a sequence of rotations given by the quaternion product of two or more quaternions and their restrictions.

Definition 4.1 (Quaternion Volume): A quaternion volume Q^\otimes is defined as

$$Q^\otimes \triangleq \{Q(\phi_1, \dots, \phi_n, \mathbf{n}_1, \dots, \mathbf{n}_n) \mid \phi_{1,\min} \leq \phi_1 \leq \phi_{1,\max} \\ \vdots \\ \phi_{n,\min} \leq \phi_n \leq \phi_{n,\max}\} \quad (7)$$

for $n \geq 1$ and where

$$Q(\phi_1, \dots, \phi_n, \mathbf{n}_1, \dots, \mathbf{n}_n) = Q(\phi_n, \mathbf{n}_n) * \dots * Q(\phi_1, \mathbf{n}_1). \quad (8)$$

In this paper, only sets of frames that can be described by a sequence of rotations about the coordinate axes are treated. We refer to [18] and [19] for a detailed discussion on quaternion volumes.

B. Reorientation of Quaternion Volumes

The quaternion product of two quaternion volumes, or a quaternion volume and a quaternion, is itself a quaternion

volume. We can use this observation to transform quaternion volumes and to represent them in a rotated coordinate system.

Let Q^\otimes be a quaternion volume and the quaternion P represent some transformation on Q^\otimes . Then, the transformation $Q_P^\otimes = Q^\otimes * P$ rotates the entire set of frames by a rotation P . Similarly, the transformation $Q_P^\otimes = Q^\otimes * P^*$ allows the set of frames represented by the quaternion volume to be represented with respect to a new reference frame P . The transformation induced by changing from one reference frame to another is called *reorientation* [20].

Proposition 4.1 (Transformation of Quaternion Volumes): Any quaternion volume Q^\otimes represented with respect to the reference frame can be transformed into another quaternion volume by

$$Q_P^\otimes = Q^\otimes * P \quad (9)$$

where the orientations represented by Q_P^\otimes relate to P in the same way as Q^\otimes relates to the reference frame.

Proof: The quaternion product $E = Q * P$ can be viewed upon as a rotation P followed by a rotation Q with respect to the *new* frame. Hence, E relates to P in the same way as Q relates to the reference frame. By the same argumentation, the quaternion volume Q_P^\otimes relates to P in the same way as Q^\otimes relates to the reference frame. ■

In Proposition 4.1, the reference frame is kept constant and the quaternion volume is rotated by P . Reorientation, however, is a rotation of the reference frame (change of observer), while the quaternion volume is kept constant. The proof of the reorientation $Q_P^\otimes = Q^\otimes * P^*$ is constructed in the same way as the proof of Proposition 4.1.

C. The Pointing Task

We now show how to represent the freedom of the pointing task as a quaternion volume. First, assume that the z axis of the end effector must be aligned with the z axis of \mathcal{F}_I . This gives the end effector one degree of rotational freedom about the z axis. The pointing task can be represented by an arbitrary rotation ψ about the z axis as the quaternion volume

$$Q_{pt}^\otimes = [\cos(\frac{\psi}{2}) \ 0 \ 0 \ \sin(\frac{\psi}{2})]^\top, \text{ for } -\pi < \psi \leq \pi. \quad (10)$$

The quaternion volume is thus given with respect to the reference frame. Assume the desired quaternion volume instead is to be rotated by $Q_d = [d_0 \ d_1 \ d_2 \ d_3]^\top$ from the reference frame. The quaternion volume that describes all orientations where the z axis points in the same direction as the z axis of Q_d is given by $Q_d^\otimes = Q_{pt}^\otimes * Q_d$ so that

$$Q_d^\otimes = \begin{bmatrix} d_0 \cos(\frac{\psi}{2}) - d_3 \sin(\frac{\psi}{2}) \\ d_1 \cos(\frac{\psi}{2}) - d_2 \sin(\frac{\psi}{2}) \\ d_2 \cos(\frac{\psi}{2}) + d_1 \sin(\frac{\psi}{2}) \\ d_3 \cos(\frac{\psi}{2}) + d_0 \sin(\frac{\psi}{2}) \end{bmatrix}, \text{ for } -\pi < \psi \leq \pi. \quad (11)$$

1) *Example 1:* If the desired orientation is chosen so that the z axis of the end effector always points in the opposite

direction of the z axis of \mathcal{F}_I by a rotation about the y axis $Q_d = [0 \ 0 \ 1 \ 0]^\top$, (11) simplifies to

$$Q_d^\otimes = [0 \ -\sin(\frac{\psi}{2}) \ \cos(\frac{\psi}{2}) \ 0]^\top, \text{ for } -\pi < \psi \leq \pi. \quad (12)$$

All quaternions that satisfy this restriction result in an end effector pointing in the opposite direction of the z axis of \mathcal{F}_I . We see this by rotating the vector $\hat{v}_z = [0 \ 0 \ 1]^\top$ by Q_d^\otimes . Then, for $-\pi < \psi \leq \pi$, we have

$$\begin{aligned} z^\otimes &= Q_d^\otimes * \mathbf{v}_z * (Q_d^\otimes)^* \\ &= \begin{bmatrix} 0 \\ -\sin(\frac{\psi}{2}) \\ \cos(\frac{\psi}{2}) \\ 0 \end{bmatrix} * \begin{bmatrix} 0 \\ 0 \\ 0 \\ 1 \end{bmatrix} * \begin{bmatrix} 0 \\ \sin(\frac{\psi}{2}) \\ -\cos(\frac{\psi}{2}) \\ 0 \end{bmatrix} \\ &= \begin{bmatrix} \cos(\frac{\psi}{2}) \sin(\frac{\psi}{2}) - \cos(\frac{\psi}{2}) \sin(\frac{\psi}{2}) \\ 0 \\ 0 \\ -\cos^2(\frac{\psi}{2}) - \sin^2(\frac{\psi}{2}) \end{bmatrix} = \begin{bmatrix} 0 \\ 0 \\ 0 \\ -1 \end{bmatrix}. \end{aligned} \quad (14)$$

D. Cone Shaped Quaternion Volumes by Rotations Sequences

A rotation sequence describes a rotation about one coordinate axis followed by a rotation about another coordinate axis in the rotated coordinate system. A general framework on how to construct easily visualizable quaternion volumes by rotation sequences is presented. We show how to construct different types of quaternion volumes and how these relate to the different rotation sequences. This will allow the programmer to choose the quaternion volume most appropriate for the task in hand or to define volumes using other rotation sequences to obtain a new shape well suited for a specific task. The rotation sequence starts with two subsequent rotations about two coordinate axes, represented by the quaternion Q_s . This defines the direction of the central axis, which is our main concern. The last degree of freedom is added by a rotation about the central axis itself, here the z axis, by Q_z . Then, the orientation of the end effector is described by

$$Q = Q_z * Q_s. \quad (15)$$

We will look into two different rotation sequences, the *ZYZ*-sequence and the *XYZ*-sequence. For the *ZYZ*-sequence, the direction of the central axis is determined by a rotation about the z axis followed by a rotation about the new y axis. Thus, the difference in the direction between the new and the old central axis is given by the rotation about the y axis only. For the *XYZ*-sequence, however, this difference is given by the first two rotations. For both sequences, the last degree-of-freedom is given by a rotation about the central axis itself and does not change its direction. Finally, the quaternion volume is given by restricting the allowed rotations of each quaternion.

We use norms in \mathbb{R}^3 to define the directions of the central axis. We consider the three cones given in Fig. 2. The cones are defined by the degree of the norm, representing the shape of the cone, and by a parameter ξ representing the size of the cone by

$$\|x_1, x_2, \dots, x_{n-1}\| \leq \xi |x_n|. \quad (16)$$

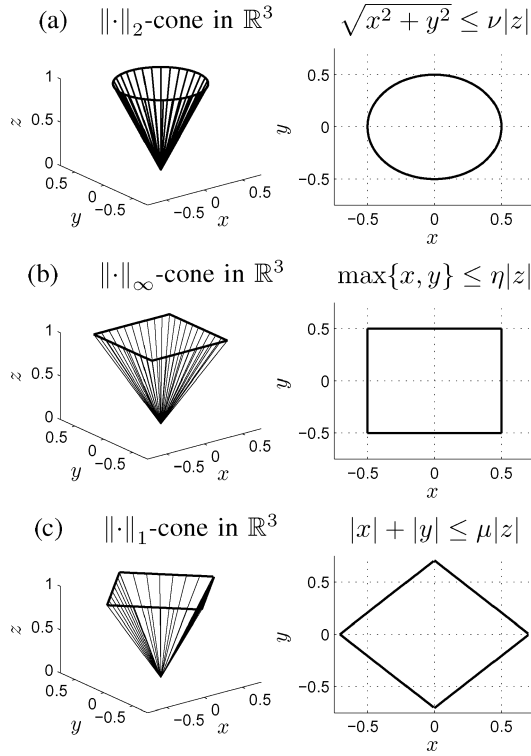


Fig. 2. Different convex cones in \mathbb{R}^3 . The cone defined by the 2-norm is self dual (setting $\mu = 1$). The cone defined by the ∞ -norm is the dual of the cone defined by the 1-norm. The illustrations of the ∞ - and 1-norms are good approximations for small rotations.

We are mainly concerned with the z axis, so in \mathbb{R}^3 , we write

$$\|x, y\| \leq \xi|z|. \quad (17)$$

1) *Example 2:* Given a $\|\cdot\|_2$ -cone with the parameter ν restricting the direction of the z axis, i.e.,

$$\sqrt{x^2 + y^2} \leq \nu|z|. \quad (18)$$

Then, the maximum rotation allowed by this cone is $\beta_{lim} = \arctan \nu$ around any axis in the xy -plane. This is obtained by the ZYZ -sequence and can be visualized in Fig. 2(a).

2) *Example 3:* Given a $\|\cdot\|_\infty$ -cone with the parameter η restricting the direction of the z axis, i.e.,

$$\max\{x, y\} \leq \eta|z|. \quad (19)$$

Then, the maximum rotation allowed by this cone is $\beta_{lim} = \arctan \eta$ around the coordinate axes (x and y axes) and $\beta_{lim} = \arctan \sqrt{2}\eta$ around the axes $x = \pm y$. This is obtained by the XYZ -sequence and can be visualized in Fig. 2(b) for small rotations.

3) *Example 4:* Given a $\|\cdot\|_1$ -cone with the parameter μ restricting the direction of the z axis, i.e.,

$$|x| + |y| \leq \mu|z|. \quad (20)$$

Then, the maximum rotation allowed by this cone is $\beta_{lim} = \arctan \mu$ around the coordinate axes (x and y axes) and $\beta_{lim} =$

$\arctan \mu/\sqrt{2}$ around the axes $x = \pm y$. This is the dual of the $\|\cdot\|_\infty$ -cone and is visualized in Fig. 2(c) for small rotations.

We note that the results are valid for rotations around globally defined x and y axes, while the XYZ -sequence rotates about the rotated coordinate axes. For the ∞ - and 1-norms this is thus an approximation and only valid for small rotations.

We will represent the desired orientations as the continuous set of directions of the central axis as described by the cones and a free rotation about the central axis itself. This set can be composed by a rotation sequence of quaternion volumes. Two rotation sequences are discussed in detail, the ZYZ -sequence, also considered in [20] and [18], and the XYZ -sequence.

4) *2-Cone:* The ZYZ -sequence allows the desired orientation to be defined as a set of vectors that span a $\|\cdot\|_2$ -cone about the reference z axis and all orientations about these vectors. Let $Q_s(\alpha, \beta) = Q(\beta, \mathbf{y}) * Q(\alpha, z)$ where $Q(\alpha, z) = [\cos(\alpha/2) \ 0 \ 0 \ \sin(\alpha/2)]^T$ and $Q(\beta, \mathbf{y}) = [\cos(\beta/2) \ 0 \ \sin(\beta/2) \ 0]^T$ so that

$$Q_s(\alpha, \beta) = \begin{bmatrix} \cos(\frac{\alpha}{2}) \cos(\frac{\beta}{2}) \\ \sin(\frac{\alpha}{2}) \sin(\frac{\beta}{2}) \\ \cos(\frac{\alpha}{2}) \sin(\frac{\beta}{2}) \\ \sin(\frac{\alpha}{2}) \cos(\frac{\beta}{2}) \end{bmatrix}. \quad (21)$$

α represents the allowed orientations about the z axis of the first rotation, while β is the allowed orientation about the new y axis. If α has no restrictions, β defines the size of a cone with the z axis at the center, illustrated in Fig. 2(a). We let γ restrict the orientation about the z axis itself and the corresponding quaternion volume is then given by

$$Q_d^\otimes = Q_z^\otimes * Q_s^\otimes = \begin{bmatrix} \cos(\frac{\beta}{2}) \cos(\frac{\gamma}{2} + \frac{\alpha}{2}) \\ \sin(\frac{\beta}{2}) \sin(\frac{\alpha}{2} - \frac{\gamma}{2}) \\ \sin(\frac{\beta}{2}) \cos(\frac{\gamma}{2} - \frac{\alpha}{2}) \\ \cos(\frac{\beta}{2}) \sin(\frac{\gamma}{2} + \frac{\alpha}{2}) \end{bmatrix} \quad (22)$$

and the restrictions

$$-\alpha_{lim} \leq \alpha \leq \alpha_{lim}, \quad (23)$$

$$0 \leq \beta \leq \beta_{lim}, \quad (24)$$

$$-\gamma_{lim} \leq \gamma \leq \gamma_{lim}. \quad (25)$$

5) *Example 5:* Assume that the central axis is to point in the opposite direction of the z axis of \mathcal{F}_I . Further assume that a small error β_{lim} in the direction is allowed and no restrictions on the rotation about the z axis. The set of frames describing these orientations is given by (22) and the restrictions

$$-\pi < \alpha \leq \pi, \quad (26)$$

$$\pi \leq \beta \leq \pi + \beta_{lim}, \quad (27)$$

$$-\pi < \gamma \leq \pi. \quad (28)$$

We can also substitute $\beta \leftarrow \pi + \beta$ and $\alpha \leftarrow -\alpha$ into (22)

$$Q_d^\otimes = Q_z^\otimes * Q_s^\otimes = \begin{bmatrix} -\sin(\frac{\beta}{2}) \cos(\frac{\gamma}{2} - \frac{\alpha}{2}) \\ \cos(\frac{\beta}{2}) \sin(\frac{\gamma}{2} + \frac{\alpha}{2}) \\ \cos(\frac{\beta}{2}) \cos(\frac{\gamma}{2} + \frac{\alpha}{2}) \\ -\sin(\frac{\beta}{2}) \sin(\frac{\alpha}{2} - \frac{\gamma}{2}) \end{bmatrix} \quad (29)$$

and restrictions (23)–(25). Note that (29) can also be obtained by rotating the quaternion volume in (22) by π radians about the y axis, i.e., by (9) with $P = [0 \ 0 \ 1 \ 0]^T$ and $Q^\otimes = [q_0 \ q_1 \ q_2 \ q_3]^T$ as in (22) so that $Q_d^\otimes = [-q_2 \ q_3 \ q_0 \ -q_1]^T$, which is the same as (29).

6) ∞ -Cone: The XYZ -sequence defines the $\|\cdot\|_\infty$ -cone, or a square cone of allowed directions where the allowed orientations about the x axis and the (new) y axis are restricted. This is a good estimation of restricting the orientation about the globally defined x - and y axes whenever the angles are kept small. $Q_s(\alpha, \beta)$ is then given by

$$Q_s(\alpha, \beta) = \begin{bmatrix} \cos(\frac{\alpha}{2}) \cos(\frac{\beta}{2}) \\ \sin(\frac{\alpha}{2}) \cos(\frac{\beta}{2}) \\ \cos(\frac{\alpha}{2}) \sin(\frac{\beta}{2}) \\ -\sin(\frac{\alpha}{2}) \sin(\frac{\beta}{2}) \end{bmatrix}. \quad (30)$$

The orientation is given by the quaternion volume

$$Q_d^\otimes = Q_z^\otimes * Q_s^\otimes \quad (31)$$

and the restrictions

$$-\alpha_{lim} \leq \alpha \leq \alpha_{lim}, \quad (32)$$

$$-\beta_{lim} \leq \beta \leq \beta_{lim}, \quad (33)$$

$$-\gamma_{lim} \leq \gamma \leq \gamma_{lim}. \quad (34)$$

E. Quaternion Volume Test

We now derive a test to verify if a quaternion lies inside the desired quaternion volume. We will in turn use this to transform these restrictions into constraints that can be handled directly in convex optimization problems. Consider a quaternion volume defined by the ZYZ -sequence. We show how to use the analytic expression of the quaternion volume to find a test to verify if a query quaternion $Q_{qry} = [q_0 \ q_1 \ q_2 \ q_3]^T$ is an element of the quaternion volume. Equation (22) gives

$$\begin{bmatrix} \cos(\frac{\beta}{2}) \cos(\frac{\gamma}{2} + \frac{\alpha}{2}) \\ \sin(\frac{\beta}{2}) \sin(\frac{\alpha}{2} - \frac{\gamma}{2}) \\ \sin(\frac{\beta}{2}) \cos(\frac{\gamma}{2} - \frac{\alpha}{2}) \\ \cos(\frac{\beta}{2}) \sin(\frac{\gamma}{2} + \frac{\alpha}{2}) \end{bmatrix} = \begin{bmatrix} q_0 \\ q_1 \\ q_2 \\ q_3 \end{bmatrix} \begin{matrix} (I) \\ (II) \\ (III) \\ (IV) \end{matrix}. \quad (35)$$

Then, from the Appendix , we get

$$\alpha = \arctan\left(\frac{q_3}{q_0}\right) + \arctan\left(\frac{q_1}{q_2}\right), \quad (36)$$

$$\beta = 2 \arcsin \sqrt{q_1^2 + q_2^2}, \quad (37)$$

$$\gamma = \arctan\left(\frac{q_3}{q_0}\right) - \arctan\left(\frac{q_1}{q_2}\right) \quad (38)$$

which gives

$$\alpha + \gamma = 2 \arctan\left(\frac{q_3}{q_0}\right). \quad (39)$$

An alternative formulation is given by [19]

$$\alpha = \arctan2\left(\frac{q_2q_3 + q_0q_1}{q_0q_2 - q_1q_3}\right) \quad (40)$$

$$\beta = 2 \arccos \sqrt{q_0^2 + q_3^2} \quad (41)$$

$$\gamma = \arctan2\left(\frac{q_2q_3 - q_0q_1}{q_0q_2 + q_1q_3}\right). \quad (42)$$

F. Transformed Quaternion Volumes

The easiest way to verify if a query quaternion lies inside a quaternion volume transformed by (9) is to transform the query quaternion by the opposite transformation P so that both the quaternion volume and the query quaternion are presented in the reference frame. Hence, the two problems below are identical.

$$Q_{qry} \in Q^\otimes * P \quad ? \quad (43)$$

$$Q_{qry} * P^* \in Q^\otimes \quad ? \quad (44)$$

This operation is computationally demanding. In the special case when an analytical expression of the transformed quaternion volume is given, as in (9), the orientation should be found by a set of parameters similar to the ones found in (40)–(42). We can obtain this when the quaternion volume is on a simple form, for example, as in (29), where the quaternion volume is rotated 180° around the y axis. Then, the query quaternion may be tested against the restrictions in (23)–(25) directly. By following the mathematics of (35)–(42), α , β and γ are found with respect to the coordinate system of $P = [0 \ 0 \ 1 \ 0]^T$ by

$$\alpha_P = \arctan2\left(\frac{q_0q_1 + q_2q_3}{q_0q_2 - q_1q_3}\right), \quad (45)$$

$$\beta_P = 2 \arcsin \sqrt{q_0^2 + q_3^2}, \quad (46)$$

$$\gamma_P = \arctan2\left(\frac{q_0q_1 - q_2q_3}{q_0q_2 + q_1q_3}\right). \quad (47)$$

Hence, as expected, we get $\beta_P = \beta - \pi$, $\alpha_P = \alpha$ and $\gamma_P = -\gamma$.

V. RESTRICTIONS ON ORIENTATION ERROR IN A CONVEX OPTIMIZATION SETTING

In this section, we show how the formalism of quaternion volumes naturally leads to formulating restrictions on the orientation as LMIs and barrier functions.

A. 2-Norm

Assume that we would like to restrict the z axis of \mathcal{F}_Q to point in approximately the same direction as the z axis of the reference frame \mathcal{F}_I . This can be visualized by a cone of directions restricted by $|\beta| \leq \beta_{lim}$ where $0 \leq \beta_{lim} \leq \pi$. The orientation error β can be found from q_1 and q_2 by (37), i.e.,

$$\beta = 2 \arcsin \sqrt{q_1^2 + q_2^2}. \quad (48)$$

A test to verify if the z axis of \mathcal{F}_Q does not deviate from the z axis of \mathcal{F}_I by more than β_{lim} is given in the following.

Proposition 5.1: Given a maximum allowed deviation in the direction of the z axis, represented by the rotation β_{lim} . Then, the z axis of \mathcal{F}_Q rotated by $Q = [q_0 \ q_1 \ q_2 \ q_3]^\top$ from the reference frame \mathcal{F}_I lies within the $\|\cdot\|_2$ -cone defined by β_{lim} if and only if

$$P = \begin{bmatrix} \eta & 0 & q_1 \\ 0 & \eta & q_2 \\ q_1 & q_2 & \eta \end{bmatrix} \succeq 0 \quad (49)$$

where $\eta = \sin \beta_{lim}/2$, $0 \leq \beta_{lim} \leq \pi$, and \succeq means positive semi-definiteness of the symmetric matrix P .

Proof: As $\eta \geq 0$ and $\eta^2 \geq 0$, from Lemma 3.1, we have that $P \succeq 0$ if $\det(P) \geq 0$. The determinant of P is given by

$$\det(P) = \eta(\eta^2 - q_1^2 - q_2^2). \quad (50)$$

Note that $0 \leq \beta_{lim} < \pi \Rightarrow \eta \geq 0$ so that $\det(P) \geq 0$ can be written as

$$\begin{aligned} \eta^2 - q_1^2 - q_2^2 &\geq 0 \\ \sin \frac{\beta_{lim}}{2} &\geq \sqrt{q_1^2 + q_2^2}. \end{aligned} \quad (51)$$

As $0 \leq \sqrt{q_1^2 + q_2^2} \leq 1 \Rightarrow 0 \leq \arcsin \sqrt{q_1^2 + q_2^2}$, we have

$$0 \leq 2 \arcsin \sqrt{q_1^2 + q_2^2} \leq \beta_{lim}. \quad (52)$$

Then, (48) concludes the proof as

$$0 \leq \beta \leq \beta_{lim}. \quad (53)$$

■

Note that the restrictions in Proposition 5.1 are on the directions of the z axis only and that rotations about the z axis itself are not restricted (the pointing task). Note also that P is symmetric and affine in Q . This is an important property as it allows us to represent the constraints as LMIs. The following follows directly from Proposition 5.1 and allows us to formulate the restrictions as a barrier function.

Corollary 5.1: Given a maximum allowed deviation in the direction of the z axis, represented by the rotation β_{lim} and let $\eta = \sin \beta_{lim}/2$. Then, the barrier function [14]

$$\phi = -\log(\eta^2 - q_1^2 - q_2^2) \quad (54)$$

increases exponentially to infinity as the orientation approaches the orientation limit forcing the z axis of \mathcal{F}_Q rotated by $Q = [q_0 \ q_1 \ q_2 \ q_3]^\top$ from the reference frame \mathcal{F}_I to lie within the restrictions given by β_{lim} .

The proof of Corollary 5.1 follows directly from the proof of Proposition 5.1.

B. ∞ -Norm

Assume instead that we would like to restrict the allowed rotation differently around different axes. For example, if the set of allowed orientations is given by restrictions on the rotation about the x axis followed by a rotation about the y axis, this

will result in a pyramid-shaped set of allowed directions. The following observations are important in this section.

Rotating the vector $\bar{\mathbf{v}}_1 = [0 \ 0 \ 1]^\top$ by α about the x axis of the reference frame followed by a rotation β about the y axis, also of the reference frame, gives the new vector

$$\bar{\mathbf{v}}_I = \begin{bmatrix} \cos \alpha \sin \beta \\ -\sin \alpha \\ \cos \alpha \cos \beta \end{bmatrix}. \quad (55)$$

For a rotation α about the x axis of the reference frame followed by a rotation β about the y axis of the rotated coordinate system, the rotated vector is given by

$$\bar{\mathbf{v}}_R = \begin{bmatrix} \sin \beta \\ -\sin \alpha \cos \beta \\ \cos \alpha \sin \beta \end{bmatrix}. \quad (56)$$

This can also be written as a quaternion Q . Let the vector $\bar{\mathbf{v}}_1$ be rotated by Q into $\mathbf{v}_2 = Q * \mathbf{v}_1 * Q^*$. Then, \mathbf{v}_2 is written as

$$\mathbf{v}_2 = \begin{bmatrix} 0 \\ 2(q_0q_2 + q_1q_3) \\ 2(q_2q_3 - q_0q_1) \\ q_0^2 - q_1^2 - q_2^2 + q_3^2 \end{bmatrix}. \quad (57)$$

Proposition 5.2: Given a restriction α_{lim} in the orientation error about the x axis of the reference frame and β_{lim} in the orientation error about the y axis of the rotated coordinate frame. Then, the z axis of \mathcal{F}_Q rotated by the quaternion $Q = [q_0 \ q_1 \ q_2 \ q_3]^\top$ with respect to the reference frame \mathcal{F}_I lies within the restrictions given by β_{lim} , where $\beta_{lim} \geq 0$, if and only if

$$P_1 = \begin{bmatrix} \eta & 0 & q_1 \\ 0 & \eta & q_0 \\ q_3 & q_2 & \eta \end{bmatrix} \succeq 0 \quad (58)$$

where $\eta = \sin \beta_{lim}/2$ and \succeq means positive semi-definiteness for the nonsymmetric matrix P_1 .

Proof: The determinant of P_1 is given by

$$\det(P_1) = \eta(\eta^2 - q_0q_2 - q_1q_3). \quad (59)$$

Assume $\det(P_1) \geq 0$

$$\begin{aligned} \eta^2 - q_0q_2 - q_1q_3 &\geq 0 \\ \sin \beta_{lim} &\geq 2(q_0q_2 + q_1q_3). \end{aligned} \quad (60)$$

As $\beta_{lim} \geq 0$, comparing (56) and (57) gives

$$\beta = \arcsin(2(q_0q_2 + q_1q_3)) \quad (61)$$

and the initial requirement is obtained by

$$\beta \leq \beta_{lim} \quad (62)$$

where β is the angle between the new z axis and the yz -plane. A similar restriction can be found for the lower bound. ■

Proposition 5.3: Given a restriction α_{lim} in the orientation error about the x axis and β_{lim} in the orientation error about the y axis, both in the reference frame. Then, the z axis of frame \mathcal{F}_Q

rotated by the quaternion $Q = [q_0 \ q_1 \ q_2 \ q_3]^T$ with respect to the reference frame \mathcal{F}_I lies within the restrictions given by α_{lim} if

$$P_2 = \begin{bmatrix} \xi & q_2q_3 & 0 \\ q_2q_3 & \xi & q_0q_1 \\ 2\xi & q_0q_1 & \xi \end{bmatrix} \succeq 0 \quad (63)$$

where $\xi = \sin \alpha_{lim}/2$.

Proof: We start with the principal minors and see that we need to add the constraint

$$\xi^2 - q_2^2q_3^2 > 0. \quad (64)$$

The determinant of P_2 is given by

$$\det(P_2) = \xi(\xi^2 - (q_0q_1)^2 - (q_2q_3)^2 + 2q_0q_1q_2q_3). \quad (65)$$

Then, $\det(P_1) \geq 0$ becomes

$$\begin{aligned} \xi^2 - (q_0q_1)^2 - (q_2q_3)^2 + 2q_0q_1q_2q_3 &\geq 0 \\ f\xi^2 &\geq (q_2q_3 - q_0q_1)^2 \\ \sin \alpha_{lim} &\geq 2|q_2q_3 - q_0q_1|. \end{aligned} \quad (66)$$

As $\alpha_{lim} \geq 0$, comparing (57) and (55) gives

$$\alpha = \arcsin(2(q_2q_3 - q_0q_1)) \quad (67)$$

and the initial requirement is obtained by

$$-\alpha_{lim} \leq \alpha \leq \alpha_{lim}. \quad (68)$$

Note that in Proposition 5.2 the second rotation is with respect to the rotated coordinate frame and the constraints restrict only the rotations about the y axis, while in Proposition 5.3 the second rotation is with respect to the rotated coordinate frame and the constraints restrict the allowed rotations about the x axis only. This simplifies the computations substantially and is a good approximation to rotating around the x and y axes of \mathcal{F}_I . We also note that the matrices given in Propositions 5.2 and 5.3 are not symmetric and that P_2 in (63) is not affine. Hence, the constraints cannot be represented as LMIs. They can, however, be represented as barrier functions given as the negative logarithm of the determinant for which we also omit the additional constraint (64).

1) *Example 6:* Given a restriction α_{lim} in the orientation error about the x axis and β_{lim} in the orientation error about the y axis. Then, the z axis of frame \mathcal{F}_Q rotated by the quaternion $Q = [q_0 \ q_1 \ q_2 \ q_3]^T$ with respect to the reference frame \mathcal{F}_Q lies within the restrictions given by α_{lim} and β_{lim} if

$$P = \begin{bmatrix} P_1 & 0 \\ 0 & P_2 \end{bmatrix} \succeq 0 \quad (69)$$

where P_1 and P_2 are given as in Propositions 5.2 and 5.3, respectively.

Alternatively, an accurate solution can be found by restricting the orientation about the x axis followed by the orientation about

the y axis, also in \mathcal{F}_I . This can be achieved by writing $\alpha = \arctan2((q_2q_3 + q_0q_1)/(q_0q_2 - q_1q_3))$ and substituting

$$\eta = \sqrt{\frac{\cos \alpha \sin \beta_{lim}}{2}} \quad (70)$$

for η in (58).

C. Restriction on the Orientation About the Central Axis

We now turn to the pointing task problem, i.e., to determine the rotation about the central axis itself. This will not change the direction of the central axis and thus not influence the orientation error. Assume we want the x axis to point in one given direction in order to improve performance. This direction may be different at every time step. Also, for the x axis, we may allow a small error from the desired direction. For the ZYZ -sequence the direction of the x axis is given by both α , β and γ . We assume the error of the direction of the z axis is restricted as in Section V-A. When this is constrained to be relatively small, the error in the direction of the x axis can be approximated by the error in the orientation about the central axis. This error is given by (39) as

$$\epsilon = \alpha + \gamma. \quad (71)$$

Proposition 5.4: Assume that the error in the direction of the z axis is small. Given a restriction in the orientation error ϵ_{lim} around the central axis, the x axis of \mathcal{F}_Q rotated by $Q = [q_0 \ q_1 \ q_2 \ q_3]^T$ from the reference frame \mathcal{F}_I lies within the restrictions given by $\epsilon_{lim} \geq 0$ if and only if

$$P = \begin{bmatrix} \kappa & \frac{q_3}{q_0} \\ \frac{q_3}{q_0} & \kappa \end{bmatrix} \succeq 0 \quad (72)$$

where $\kappa = \tan \epsilon_{lim}/2$.

Proof: The determinant of P is given by

$$\det(P) = \kappa^2 - \frac{q_3^2}{q_0^2}. \quad (73)$$

As ϵ_{lim} is positive, we have $0 \leq \tan \epsilon_{lim}/2$ for $0 \leq \epsilon_{lim} \leq \pi$ and $\det(P) \geq 0$ can be written as

$$\begin{aligned} \kappa^2 &\geq \frac{q_3^2}{q_0^2} \\ \epsilon_{lim} &\geq \left| 2 \arctan \left(\frac{q_3}{q_0} \right) \right|. \end{aligned} \quad (74)$$

Then, (39) concludes that

$$-\epsilon_{lim} \leq \epsilon \leq \epsilon_{lim}. \quad (75)$$

Also, for Proposition 5.4, we can reformulate the result and obtain a barrier function.

Corollary 5.2: Assume that the orientation error of the direction of the z axis is small and the orientation error about the

central axis is restricted to ϵ_{lim} and let $\kappa = \tan(\epsilon_{lim}/2)$. Then, the barrier function

$$\phi = -\log\left(\kappa^2 - \frac{q_3^2}{q_0^2}\right) \quad (76)$$

increases exponentially to infinity as the orientation approaches the orientation limit, forcing the x axis of \mathcal{F}_Q rotated by $Q = [q_0 \ q_1 \ q_2 \ q_3]^T$ from the reference frame \mathcal{F}_I to lie within the restrictions given by ϵ_{lim} .

D. Direction of the x Axis

Alternatively, one might want to restrict the direction of the x axis directly. Note that the matrix given in the previous section is not affine and cannot be written as an LMI. Hence, another matrix that is both symmetric and affine is proposed in the following. Assume that the direction of the x axis is to be restricted. Similarly to (49), the requirement that the body frame x axis is to point in the direction of the reference frame x axis is given by

$$P_2 = \begin{bmatrix} \xi & 0 & q_2 \\ 0 & \xi & q_3 \\ q_2 & q_3 & \xi \end{bmatrix} \succeq 0 \quad (77)$$

where $\xi = \sin \epsilon_{lim}/2$. This will restrict the x axis of \mathcal{F}_Q to lie within a cone with the x axis of \mathcal{F}_I at the center.

This quaternion volume can also be transformed by (9). Assume that the direction of the body frame x axis is to point in the direction given by the direction of the x axis of $Q_d = [d_0 \ d_1 \ d_2 \ d_3]^T$. In order to apply the restriction given by (77), but to the direction of the x axis of \mathcal{F}_{Q_d} and not that of \mathcal{F}_I , Q is transformed back into the reference frame and the test is performed on the transformed quaternion

$$Q_t = Q * Q_d^* = \begin{bmatrix} * & * & * \\ -q_0 d_2 + q_2 d_0 & -q_3 d_1 + q_1 d_3 & * \\ -q_0 d_3 + q_3 d_0 & -q_1 d_2 + q_2 d_1 & * \end{bmatrix}. \quad (78)$$

Note that when Q_t is substituted into (77), P_2 is still symmetric and affine in Q .

VI. SPRAY PAINTING

We now present an example where the direction of the z axis is determined by two cone-shaped sets of orientations. The direction given by the two sets at each time step is in general conflicting and the solution is the minimum of a cost function given by the sum of the two orientation errors. There are two main criteria that will guarantee uniform paint coating, the orientation of the spray gun with respect to the surface and its velocity. The first restriction is ensured by the constraint

$$\eta^2 - q_1^2 - q_2^2 > 0 \quad (79)$$

where $\eta = \sin(\beta_{lim}/2)$ and β_{lim} is the maximum allowed orientation error for which the quality of the paint job is satisfying. The paint gun should always be orthogonal to the surface, but in general an orientation error of about 20° guarantees uniform paint coating. We will assume a manipulator that is to paint a

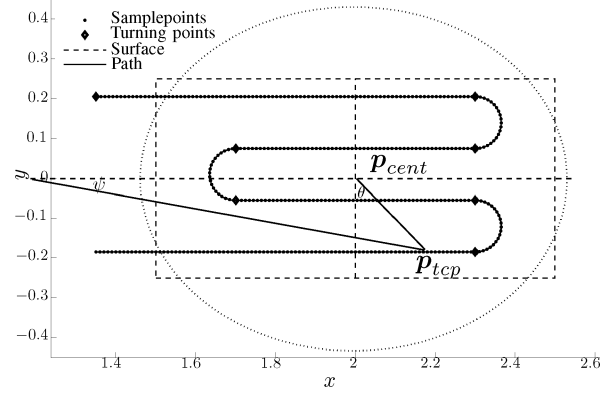


Fig. 3. The path of the tool center point (TCP) in the xy -plane. The direction of the central axis is determined from θ by the quaternion $Q_d(\theta)$ and the rotation around the central axis itself is determined from ψ .

surface in the xy -plane following the path in Fig. 3. The restrictions on the orientation is visualized by a cone. The cross section of this cone is given by the circle in Fig. 3.

The second restriction is on the velocity of the paint gun and can be improved by a similar constraint. The general idea is to reduce the displacement of the paint gun by choosing a desired orientation at each time step which forces the position of the paint gun to remain at the center of the surface. This will reduce the torques in the main axes as these are mainly used for positioning the end effector. Assume we want to paint the surface in the xy -plane with a constant distance z_{des} between the tool and the surface. Let \mathbf{c} be the vector from the center of the surface, at height z_{des} , denoted \mathbf{p}_{cent} , to the current position \mathbf{p}_{tcp} on the surface

$$\mathbf{c} = \mathbf{p}_{tcp} - \mathbf{p}_{cent}. \quad (80)$$

This is the direction of the central axis for which the main axes do not need to move at all, i.e., pure rotation of the wrist. We choose this as the desired direction of the central axis when the orientation error is not considered, represented by Q_d . We now introduce the same freedom in this constraint as we did with the orientation error, forcing the orientation to lie inside a quaternion volume with the z axis of Q_d at the center.

First, we transform the quaternion back into the reference frame and perform the test on the transformed quaternion in the reference frame. The transformed quaternion is given by

$$Q_p(t) = \begin{bmatrix} p_0 \\ p_1 \\ p_2 \\ p_3 \end{bmatrix} = Q * Q_d^*(t) = \begin{bmatrix} * & * & * \\ -q_0 d_1 + q_1 d_0 & -q_2 d_3 + q_3 d_2 \\ -q_0 d_2 + q_2 d_0 & -q_3 d_1 + q_1 d_3 \\ * & * & * \end{bmatrix}. \quad (81)$$

The constraint that forces the end effector to point in the direction of Q_d with a maximum orientation error α_{lim} is given by Proposition 5.1 as

$$\xi^2 - p_1^2 - p_2^2 > 0 \quad (82)$$

where $\xi = \sin(\alpha_{lim}/2)$. Thus, we use the same constraint as for the reference frame, but on the transformed quaternion $Q_p(t)$.

We now turn to the problem of spray painting the surface in the xy -plane in Fig. 3, also addressed in [10]. The surface is to be painted from above, so the set representing the orientation error needs to be rotated 180° so that it points downwards. This can be done by (9) with $P = [0 \ 0 \ 1 \ 0]^T$ or the approach that we will take here, instead of the restriction $\eta^2 \geq q_1^2 + q_2^2$, which we used in Proposition 5.1, we write

$$\eta^2 \leq q_1^2 + q_2^2 \quad (83)$$

and replace $\beta_{lim} \leftarrow \pi - \beta_{lim}$ in $\eta = \sin(\beta_{lim}/2)$. This will guarantee that the set of orientations points in exactly the opposite direction of the set of (82). The barrier function is then the sum of the two constraints representing the orientation error and the velocity and is given by

$$\begin{aligned} \phi &= k_{err}\phi_{err} + k_{tcp}\phi_{tcp} \\ &= -k_{err}\log(q_1^2 + q_2^2 - \eta^2) - k_{tcp}\log(\xi^2 - p_1^2 - p_2^2) \end{aligned} \quad (84)$$

where ϕ_{err} guarantees that the orientation error lies within the limits and ϕ_{tcp} allows the end effector to follow the path with a higher velocity. The weights k_{err} and k_{tcp} weighs the importance of the two restrictions and should be chosen so that the end-effector velocity is constant and as high as possible.

A. The Gradient Method and Implementation

In this section, we show how to solve the optimization problem by the gradient method. The partial derivatives are given by

$$\frac{\partial \phi_{err}}{\partial q_0} = 0, \quad \frac{\partial \phi_{err}}{\partial q_1} = -\frac{2q_1}{q_1^2 + q_2^2 - \eta^2} \quad (85)$$

$$\frac{\partial \phi_{err}}{\partial q_3} = 0, \quad \frac{\partial \phi_{err}}{\partial q_2} = -\frac{2q_2}{q_1^2 + q_2^2 - \eta^2} \quad (86)$$

and

$$\frac{\partial \phi_{tcp}}{\partial q_0} = -\frac{2(d_1^2 + d_2^2)q_0 - 2(d_0d_1 + d_2d_3)q_1 + 2(d_1d_3 - d_0d_2)q_2}{\xi^2 - p_1^2 - p_2^2}$$

$$\frac{\partial \phi_{tcp}}{\partial q_1} = -\frac{2(d_0^2 + d_3^2)q_1 - 2(d_0d_1 + d_2d_3)q_0 + 2(d_0d_2 - d_1d_3)q_3}{\xi^2 - p_1^2 - p_2^2}$$

$$\frac{\partial \phi_{tcp}}{\partial q_2} = -\frac{2(d_0^2 + d_3^2)q_2 + 2(d_1d_3 - d_0d_2)q_0 - 2(d_2d_3 + d_0d_1)q_3}{\xi^2 - p_1^2 - p_2^2}$$

$$\frac{\partial \phi_{tcp}}{\partial q_3} = -\frac{2(d_1^2 + d_2^2)q_3 + 2(d_0d_2 - d_1d_3)q_1 - 2(d_2d_3 + d_0d_1)q_2}{\xi^2 - p_1^2 - p_2^2}$$

The gradient is then given by

$$\nabla \phi = \begin{bmatrix} k_{err}\frac{\partial \phi_{err}}{\partial q_0} + k_{tcp}\frac{\partial \phi_{tcp}}{\partial q_0} \\ k_{err}\frac{\partial \phi_{err}}{\partial q_1} + k_{tcp}\frac{\partial \phi_{tcp}}{\partial q_1} \\ k_{err}\frac{\partial \phi_{err}}{\partial q_2} + k_{tcp}\frac{\partial \phi_{tcp}}{\partial q_2} \\ k_{err}\frac{\partial \phi_{err}}{\partial q_3} + k_{tcp}\frac{\partial \phi_{tcp}}{\partial q_3} \end{bmatrix}. \quad (87)$$

The problem is solved by the gradient method

$$\phi^{k+1} = \phi^k - a\nabla\phi. \quad (88)$$

For a feasible initial condition and for a relatively small and constant step size a the stability and convergence of the method is good. Due to the low computational burden of this approach, a constant step is used instead of a search. This requires that a is chosen conservatively which may lead to slower convergence.

B. The Pointing Task

By the approach described in the previous section, the orientation about the central axis (z axis) is not determined. In this section, we show how to utilize the last degree of freedom to improve performance further. We will present three different approaches for implementing the solution to the pointing task problem. The orientations found do not differ very much, but the implementations are quite different.

1) *From and Gradvahl [10]*: The first approach presented is the intuitive approach given in [10]. The orientation about the central axis at point i is set as

$$\psi(t) = k_\psi \arctan 2 \left(\frac{y(t)}{x(t) - x_{cent}} \right) \quad (89)$$

for $k_\psi \in (0, 1]$ and where $x(t)$ and $y(t)$ give the position of the end effector at time t in the xy -plane and x_{cent} is the center of the surface in the x -direction. $\psi(t)$ is shown in Fig. 3. It was shown by From and Gradvahl [10] that this will reduce the displacement of the main axes.

2) *Direction of the x Axis (Section V-D)*: A similar approach is to force the end effector x axis to point in the direction of the base of the manipulator. By projecting the end-effector x axis into the xy -plane and force this to point in the direction of the base will have approximately the same effect as the approach in the previous section, but this constraint can easily be written on the form of (78) as

$$\begin{aligned} Q_r(t) &= \begin{bmatrix} r_0 \\ r_1 \\ r_2 \\ r_3 \end{bmatrix} = Q * Q_e^*(t) \\ &= \begin{bmatrix} * \\ * \\ -q_0e_2 + q_2e_0 - q_3e_1 + q_1e_3 \\ -q_0e_3 + q_3e_0 - q_1e_2 + q_2e_1 \end{bmatrix} \end{aligned} \quad (90)$$

where $Q_e(t)$ is time varying and takes the end-effector x axis into the desired direction. Further, we want the end-effector x axis to point in the opposite direction of the global x axis, so we let $\gamma_{lim} \leftarrow \pi - \gamma_{lim}$ and write the corresponding cost function as

$$\phi_x = -\log(r_2^2 + r_3^2 - \nu^2) \quad (91)$$

where $\nu = \sin(\gamma_{lim}/2)$ and γ_{lim} is the maximum error allowed in the direction of the x axis. The partial derivatives are given by

$$\begin{aligned}\frac{\partial \phi_x}{\partial q_0} &= -\frac{2(e_2^2 + e_3^2)q_0 - 2(e_0e_2 + e_1e_3)q_2 + 2(e_1e_2 - e_0e_3)q_3}{r_2^2 + r_3^2 - \nu^2} \\ \frac{\partial \phi_x}{\partial q_1} &= -\frac{2(e_2^2 + e_3^2)q_1 + 2(e_0e_3 - e_1e_2)q_2 - 2(e_1e_3 + e_0e_2)q_3}{r_2^2 + r_3^2 - \nu^2} \\ \frac{\partial \phi_x}{\partial q_2} &= -\frac{2(e_0^2 + e_1^2)q_2 - 2(e_0e_2 + e_1e_3)q_0 + 2(e_0e_3 - e_1e_2)q_1}{r_2^2 + r_3^2 - \nu^2} \\ \frac{\partial \phi_x}{\partial q_3} &= -\frac{2(e_0^2 + e_1^2)q_3 + 2(e_1e_2 - e_0e_3)q_0 - 2(e_1e_3 + e_0e_2)q_1}{r_2^2 + r_3^2 - \nu^2}.\end{aligned}$$

Thus, the search direction for every time step is given by

$$\nabla \phi = \begin{bmatrix} k_{err} \frac{\partial \phi_{err}}{\partial q_0} + k_{tcp} \frac{\partial \phi_{tcp}}{\partial q_0} + k_x \frac{\partial \phi_x}{\partial q_0} \\ k_{err} \frac{\partial \phi_{err}}{\partial q_1} + k_{tcp} \frac{\partial \phi_{tcp}}{\partial q_1} + k_x \frac{\partial \phi_x}{\partial q_1} \\ k_{err} \frac{\partial \phi_{err}}{\partial q_2} + k_{tcp} \frac{\partial \phi_{tcp}}{\partial q_2} + k_x \frac{\partial \phi_x}{\partial q_2} \\ k_{err} \frac{\partial \phi_{err}}{\partial q_3} + k_{tcp} \frac{\partial \phi_{tcp}}{\partial q_3} + k_x \frac{\partial \phi_x}{\partial q_3} \end{bmatrix}. \quad (92)$$

Applying the gradient method will find the minimum of a cost function given by the sum of three in general conflicting objectives. ϕ_{err} guarantees that the orientation error is within its limits, ϕ_{tcp} increases the velocity of the paint gun and ϕ_x exploits the pointing task to increase the velocity further.

3) *Restrictions of the Rotation About the Central Axis (Section V-C)*: By Proposition 5.4, we get that the rotation about the z axis can be forced to zero by the cost function

$$\phi_x = -k_x \log \left(\kappa^2 - \frac{q_3^2}{q_0^2} \right). \quad (93)$$

The partial derivatives are given by

$$\begin{aligned}\frac{\partial \phi_x}{\partial q_1} &= 0, \quad \frac{\partial \phi_x}{\partial q_0} = -\frac{2q_3^2}{q_0(\kappa^2 q_0^2 - q_3^2)}, \\ \frac{\partial \phi_x}{\partial q_2} &= 0, \quad \frac{\partial \phi_x}{\partial q_3} = \frac{2q_3}{\kappa^2 q_0^2 - q_3^2}.\end{aligned}$$

We would like the x axis to point in the direction of the base, which we obtain by a rotation about the z axis by $Q_e = [e_0 \ 0 \ 0 \ e_3]^T$. Again, we use $Q_r = Q * Q_e^*$ and

$$\phi_x = -\log \left(\kappa^2 - \frac{r_3^2}{r_0^2} \right) \quad (94)$$

where

$$Q_r(t) = \begin{bmatrix} r_0 \\ r_1 \\ r_2 \\ r_3 \end{bmatrix} = Q * Q_e^*(t) = \begin{bmatrix} q_0 e_0 + q_3 e_3 \\ * \\ * \\ -q_0 e_3 + q_3 e_0 \end{bmatrix}. \quad (95)$$

The partial derivatives are then given by

$$\begin{aligned}\frac{\partial \phi_x}{\partial q_1} &= 0, \quad \frac{\partial \phi_x}{\partial q_2} = 0 \\ \frac{\partial \phi_x}{\partial q_0} &= \frac{2(e_3^4 - e_0^4)q_0 q_3^2 - 2(q_3^3 - q_0^2 q_3)(e_0^3 e_3 + e_0 e_3^3)}{r_0^2(\kappa^2 r_0^2 - r_3^2)} \\ \frac{\partial \phi_x}{\partial q_3} &= \frac{2(e_0^4 - e_3^4)q_0^2 q_3 - 2(q_0^3 - q_0 q_3^2)(e_0 e_3^3 + e_0^3 e_3)}{r_0^2(\kappa^2 r_0^2 - r_3^2)}.\end{aligned} \quad (96)$$

Then, by choosing Q_e such that the x axis points in the direction of the base by a rotation about the z axis, we obtain the desired motion characteristics. Note that in (94) the central axis is assumed to be orthogonal to the surface. Hence, the results are only valid when a small orientation error in the direction of the z axis is allowed.

C. LMIs

We now turn to the problem of how to formulate the constraints on the orientation as LMIs and how to solve this when several constraints are present. The problem

$$\begin{aligned}\text{minimize} \quad & \phi(x) = \log \det G(x)^{-1} \\ \text{subject to} \quad & G(x) \succ 0\end{aligned} \quad (97)$$

where

$$G(x) = G_0 + x_1 G_1 + x_2 G_2 + \dots + x_m G_m \quad (98)$$

is known as the analytic centering problem. This formulation allows us to formulate the restrictions on the z and x axes in one big block diagonal matrix and solve this very efficiently. If the feasible set $\mathbf{X} = \{x \mid G(x) \succ 0\}$ is nonempty and bounded, the matrices $G_i, i = 1, \dots, m$ are linearly independent and the objective function is strictly convex on \mathbf{X} [13]. In this case, it can be guaranteed that the optimality condition $\nabla \phi(x^*) = 0$, for an optimal solution x^* , can be reached.

In our case, the constraints on the z axis are written as

$$\begin{aligned}\text{minimize} \quad & \phi(x) = \log \det P(x)^{-1} \\ \text{subject to} \quad & P(x) \succ 0\end{aligned} \quad (99)$$

where P is given by (49) and can be written as

$$P(x) = P_0 + x_1 P_1 + x_2 P_2 + x_3 P_3 + x_4 P_4, \quad (100)$$

where

$$\begin{aligned}x_1 &= q_0, \quad x_2 = q_1, \quad x_3 = q_2, \quad x_4 = q_3, \\ P_0 &= \begin{bmatrix} \eta & 0 & 0 \\ 0 & \eta & 0 \\ 0 & 0 & \eta \end{bmatrix}, \quad P_1 = P_4 = \begin{bmatrix} 0 & 0 & 0 \\ 0 & 0 & 0 \\ 0 & 0 & 0 \end{bmatrix}, \\ P_2 &= \begin{bmatrix} 0 & 0 & 1 \\ 0 & 0 & 0 \\ 1 & 0 & 0 \end{bmatrix}, \quad P_3 = \begin{bmatrix} 0 & 0 & 0 \\ 0 & 0 & 1 \\ 0 & 1 & 0 \end{bmatrix}.\end{aligned} \quad (101)$$

q_0 and q_3 do not affect the solution and can be eliminated from the equations.

To apply the time varying constraints on the transformed x axis, substitute (78) into (77), denote the resulting matrix F , and write it on the form of (100) so that

$$F(x) = F_0 + x_1 F_1 + x_2 F_2 + x_3 F_3 + x_4 F_4, \quad (102)$$

$$x_1 = q_0, \quad x_2 = q_1, \quad x_3 = q_2, \quad x_4 = q_3$$

$$F_0 = \begin{bmatrix} \xi & 0 & 0 \\ 0 & \xi & 0 \\ 0 & 0 & \xi \end{bmatrix}, \quad F_1(t) = \begin{bmatrix} 0 & 0 & -d_2 \\ 0 & 0 & -d_3 \\ -d_2 & -d_3 & 0 \end{bmatrix}$$

$$F_2(t) = \begin{bmatrix} 0 & 0 & -d_3 \\ 0 & 0 & d_2 \\ -d_3 & d_2 & 0 \end{bmatrix}, \quad F_3(t) = \begin{bmatrix} 0 & 0 & d_0 \\ 0 & 0 & -d_1 \\ d_0 & -d_1 & 0 \end{bmatrix}$$

$$F_4(t) = \begin{bmatrix} 0 & 0 & d_1 \\ 0 & 0 & d_0 \\ d_1 & d_0 & 0 \end{bmatrix}. \quad (103)$$

To combine the restrictions of the x and z axes, we use Lemma 3.2 and formulate the problem as

$$\text{minimize } \phi(x) = \log \det \begin{bmatrix} P(x) & 0 \\ 0 & F(x) \end{bmatrix}^{-1}$$

$$\text{subject to } \begin{bmatrix} P(x) & 0 \\ 0 & F(x) \end{bmatrix} \succ 0 \quad (104)$$

for which the solution is the orientation which minimizes the error both of the x axis and the z axis with a “metric” that increases exponentially with the angular distance from the desired directions of the x and z axes. Also note that for two conflicting constraints on the direction of the z axis, the constraints given by (82) can be written similarly by substituting (81) into (49).

D. Normalization

The optimization algorithms described optimize freely over all quaternions, and it is thus not guaranteed, nor likely, that the resulting quaternion is of unit length. One simple and very effective, though not very mathematically sound solution, is to optimize freely over all quaternions and then normalize the result afterwards. This turns out to work very well in practice. Another option is to add the constraint $|Q| = 1$ in the optimization algorithm which guarantees that the search space is only the set of quaternions of unit length.

E. Optimality and Existence of the Solutions

We note that the quaternion volumes must be chosen so that a solution exists. The quaternion volume representing the orientation error should be chosen according to the maximum allowed error. For the quaternion volume constructed to increase velocity, we have more freedom in choosing the size of the volume. This should thus be chosen big enough so that a solution always exists. This can then be compensated for by increasing k_{tcp} in (84) or (87).

The optimal orientation at every time step can be found in real time given the velocity of the paint gun. However, the optimal velocity is not found in real time. This is achieved by increasing the velocity until the simulations show that the joint torques reach the limits. Thus, to find the optimal velocity, we

need to perform several simulations or test runs to find this. In this sense, the solution is not found in real time. On the other hand, if the manipulator is to follow a trajectory for which the maximum velocity is not found by test runs, we can use information about the curvature of the path and the maximum orientation error to choose a velocity that is far higher than for the conventional approach. In this sense, the solution is optimal for the chosen velocity. The main strength of this method lies in its simplicity. The low computation time allows us to run the problem several times to find a solution very close to the optimal one. There are many alternative approaches well suited to find an optimal or closer to optimal solution. A learning approach may find a more optimal solution, but this would require far more computational effort. One might also construct an optimization problem that optimizes the torques given a freedom in the orientation, but to find an optimal global solution to this problem is extremely complicated. The short computation time for the proposed algorithm makes it a good alternative to the computationally more demanding approaches.

F. Curved Surfaces

The approach presented is not limited to planar surfaces. For curved surfaces such as the hood of a car, we can use the exact same approach. The desired direction of the end effector used in (81) can be chosen as the same as the planar case. However, the quaternion volume representing the orientation error must be transformed similarly to (81) so that the center of the volume is orthogonal to the surface at every point on the trajectory. For curved surfaces, we expect the performance to improve more than for a plane as the orientation of the paint gun does not have to follow the optimal orientation (orthogonal to the surface) as tightly and can sweep over the surface more smoothly and with less variation in the orientation.

VII. NUMERICAL EXAMPLES

A. Convergence

Table I shows the computational efficiency of the algorithms presented. The convergence is in general very good and a solution is found in 10–20 iterations. In some cases, a few more iterations are needed, but for all the tests performed, about 50 iterations is sufficient, as a worst-case measure. No information from the previous solution is used in choosing the initial conditions. The simulations were performed on an Intel T7200 2 GHz processor. We can see that the time needed for each iteration is very low. Even for the worst case of 50 iterations, the time needed to find a solution is less than one millisecond. This makes all the algorithms presented suitable for online implementation.

The three algorithms presented were compared in terms of computational efficiency. The algorithms tested were: i) z axis cone restrictions as presented in Section VI-A; ii) z axis cone restrictions as presented in Section VI-A with additional cone restriction on the direction of the x axis as presented in Section VI-B2; and iii) z axis cone restrictions as presented in Section VI-A with additional restriction on the rotation about the z axis, as presented in Section VI-B3.

TABLE I
SPEED FOR ONE ITERATION, NUMBER OF ITERATIONS NEEDED TO “GUARANTEE” AN OPTIMAL SOLUTION (WORST CASE), AND TIME NEEDED TO OBTAIN OPTIMAL SOLUTION

Algorithm	Iteration time [ms]	Max its needed	Max time [ms]
i) z -axis cone	0.00232	50	0.116
ii) z -axis cone & x -axis cone	0.00268	50	0.1608
iii) z -axis cone & restr x -axis	0.00605	50	0.363

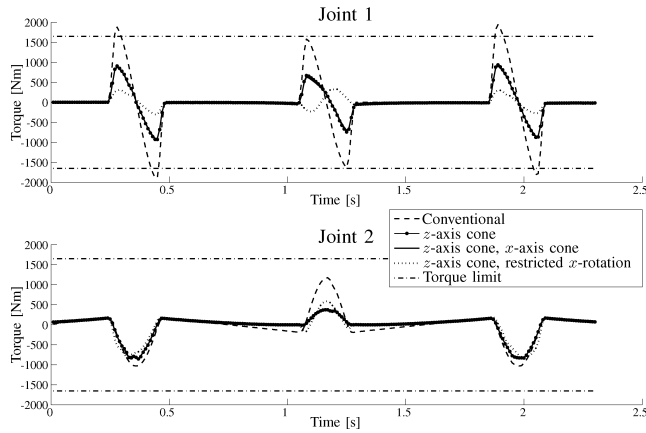


Fig. 4. Torques for joint 1 and 2 for the four different approaches presented.

B. Trajectory Speed

The same algorithms were tested for trajectory following. The manipulator was to follow the path given in Fig. 3 with a constant speed of 1 m/s. The torques of joints 1 and 2 for each case is shown in Fig. 4 together with the torque limits of each joint. We can see that all the approaches improve performance substantially. The approach that only adds constraints on the direction of the z axis performs very well and is very easy to implement. For large allowed orientation errors of the z axis, the x axis cone will reduce the orientation error not only of the x axis but also the z axis. This may be considered a side-effect of this cone constraint as the main motivation behind this restriction is to change the direction of the x axis and not the z axis. This side-effect is not present for the last approach which determines the direction of the x axis by restricting the rotation around the end-effector z axis. This approach will thus perform better in some cases as the orientation error of the z axis, which is our main concern, is not reduced. This approach does, however, have a numerical singularity when q_0 approaches zero. This must be handled in the implementation.

Table II shows the maximum speed for which the manipulator can follow the path for each algorithm. The speed increases for all the approaches presented. Table II also shows the maximum orientation error of the z axis in each case. The maximum allowed orientation error is set to 20° for all approaches. We see that the maximum orientation error when both the z and x axes are restricted by a cone is lower than for the two other cases. This is because, as described above, the restriction on the x axis cone will also affect direction of the z axis. As the direction

TABLE II
THE MAXIMUM SPEED THE MANIPULATOR CAN FOLLOW THE PATH FOR THE FOUR DIFFERENT APPROACHES AND THE CORRESPONDING ORIENTATION ERRORS

Algorithm	Max vel [m/s]	Max or. error [$^\circ$]
Conventional	0.91	0
i) z -axis cone	1.35	20
ii) z -axis cone & x -axis cone	1.28	12
iii) z -axis cone & restr x -axis	1.37	20

of the z axis is our main tool to improve performance, this approach does not perform as well as the other two when large orientation errors are allowed.

VIII. CONCLUSION

In this paper, we have shown how to transform a constraint on a continuous set of orientations into a convex constraint. By representing the constraints as LMIs or barrier functions the optimal solution for a given cost function can be found in real time at every time step. For spray paint applications this allows us to exploit the fact that a small orientation error can be utilized to increase the velocity of the paint gun during turn, guaranteeing uniform paint coating and substantially decreasing the time needed to paint a surface.

APPENDIX

The quaternion volume is given by (22), i.e.,

$$\begin{bmatrix} \cos(\frac{\beta}{2}) \cos(\frac{\gamma}{2} + \frac{\alpha}{2}) \\ \sin(\frac{\beta}{2}) \sin(\frac{\gamma}{2} - \frac{\alpha}{2}) \\ \sin(\frac{\beta}{2}) \cos(\frac{\gamma}{2} - \frac{\alpha}{2}) \\ \cos(\frac{\beta}{2}) \sin(\frac{\gamma}{2} + \frac{\alpha}{2}) \end{bmatrix} = \begin{bmatrix} q_0 \\ q_1 \\ q_2 \\ q_3 \end{bmatrix} \begin{matrix} (I) \\ (II) \\ (III) \\ (IV) \end{matrix}. \quad (109)$$

By substituting (II) into (III), (III) becomes

$$\sin(\frac{\beta}{2}) \sqrt{1 - \frac{q_1^2}{\sin^2(\frac{\beta}{2})}} = q_2 \quad (110)$$

and $\beta = 2 \arcsin \sqrt{q_1^2 + q_2^2}$ is positive by definition. α and γ are found by dividing (II) by (III) and (IV) by (I)

$$\tan\left(\frac{\alpha}{2} - \frac{\gamma}{2}\right) = \frac{q_1}{q_2}, \quad \tan\left(\frac{\gamma}{2} + \frac{\alpha}{2}\right) = \frac{q_3}{q_0}. \quad (111)$$

We write

$$\frac{\alpha}{2} - \frac{\gamma}{2} = \arctan\left(\frac{q_1}{q_2}\right), \quad \frac{\gamma}{2} + \frac{\alpha}{2} = \arctan\left(\frac{q_3}{q_0}\right) \quad (112)$$

so that α , β , and γ are given by (36)–(38).

REFERENCES

- [1] S.-H. Suh, I.-K. Woo, and S.-K. Noh, “Development of an automatic trajectory planning system (ATPS) for spray painting robots,” in *Proc. IEEE Int. Conf. Robot. Autom.*, CA, 1991, pp. 209–216.
- [2] R. Ramabhadran and J. Antonio, “Fast solution techniques for a class of optimal trajectory planning problems with applications to automated spray coating,” *IEEE Trans. Robot. Autom.*, vol. 13, no. 4, pp. 519–530, 1997.
- [3] J. K. Antonio, “Optimal trajectory planning for spray coating,” in *Proc. IEEE Int. Conf. Robot. Autom.*, CA, 1994, pp. 2570–2577.

- [4] T. Kim and S. E. Sarma, "Optimal sweeping paths on a 2-manifold: A new class of optimization problems defined by path structures," *IEEE Trans. Robot. Autom.*, vol. 19, no. 4, pp. 613–636, 2003.
- [5] P. Hertling, L. Hog, R. Larsen, J. Perram, and H. Petersen, "Task curve planning for painting robots-Part 1: Process modeling and calibration," *IEEE Trans. Robot. Autom.*, vol. 12, no. 2, pp. 324–330, 1996.
- [6] D. Conner, A. Greenfield, P. Atkar, A. Rizzi, and H. Choset, "Paint deposition modeling for trajectory planning on automotive surfaces," *Autom. Sci. Eng.*, vol. 2, no. 4, pp. 381–392, 2005.
- [7] T. S. Smith, R. T. Farouki, M. al Kandari, and H. Pottmann, "Optimal slicing of free-form surfaces," *Comput. Aided Geometric Design*, vol. 19, no. 1, pp. 43–64, 2001.
- [8] P. N. Atkar, A. Greenfield, D. C. Conner, H. Choset, and A. A. Rizzi, "Uniform coverage of automotive surface patches," *Int. J. Robot. Res.*, vol. 24, no. 11, pp. 883–898, 2005.
- [9] V. Potkonjak, G. Dordevic, D. Kostic, and M. Rasic, "Dynamics of anthropomorphic painting robot: Quality analysis and cost reduction," *Robot. Autom. Syst.*, vol. 32, no. 1, pp. 17–38, 2000.
- [10] P. J. From and J. T. Gravdahl, "General solutions to kinematic and functional redundancy," in *Proc. 46th IEEE Conf. Decision Control*, LA, 2007, pp. 5779–5786.
- [11] M. Buss, H. Hashimoto, and J. Moore, "Dextrous hand grasping force optimization," *IEEE Trans. Robot. Autom.*, vol. 12, no. 3, pp. 406–418, 1996.
- [12] P. J. From and J. T. Gravdahl, "On the equivalence of orientation error and positive definiteness of matrices," in *Proc. Int. Conf. Control, Autom., Robot. Vision*, Kobe, Japan, 2008, pp. 2089–2094.
- [13] L. Vandenberghe, S. Boyd, and S.-P. Wu, "Determinant maximization with linear matrix inequality constraints," 1996. [Online]. Available: <http://stanford.edu/~boyd/papers/maxdet.html>
- [14] S. Boyd and L. Vandenberghe, *Convex Optimization*. Cambridge, U.K.: Cambridge Univ. Press, 2004.
- [15] S. Boyd, L. E. Ghaoui, E. Feron, and V. Balakrishnan, *Linear Matrix Inequalities in System and Control Theory*. Philadelphia, PA: Studies in Applied Mathematics, 1994, vol. 15.
- [16] J. B. Kuipers, *Quaternions and Rotation Sequences*. Princeton, NJ: Princeton Univ. Press, 2002.
- [17] J. C. van der Ha and M. Shuster, "A tutorial on vectors and attitude," *IEEE Control Syst. Mag.*, vol. 29, no. 2, pp. 94–107, 2009.
- [18] A. J. Hanson, *Visualizing Quaternions*. San Francisco, CA: Morgan Kaufmann, 2006.
- [19] P. J. From and J. T. Gravdahl, "Representing attitudes as sets of frames," in *Proc. Amer. Control Conf.*, 2007, pp. 2465–2472.
- [20] B. Alpern, L. Carter, M. Grayson, and C. Pelkie, "Orientation maps: Techniques for visualizing rotations (A consumers guide)," in *Proc. IEEE Conf. Visualization*, CA, 1993, pp. 183–188.



Pål Johan From (M'05) received the M.Sc. degree in engineering cybernetics from the Norwegian University of Science and Technology, Trondheim, Norway, in 2006. He is currently working towards the Ph.D. degree in engineering cybernetics at the Norwegian University of Science and Technology.

He now works in the TAIL IO R&D Consortium where he does research in the field of robotics and automation on offshore installations. His research interests include modeling and control of robotic manipulators, open and closed chain kinematics, industrial manipulators, and offshore robotics.



Jan Tommy Gravdahl (S'94–M'98–SM'04) received the Siv.Ing degree in 1994 and the Dr.Ing. degree in 1998 in engineering cybernetics from the Norwegian University of Science and Technology (NTNU), Trondheim, Norway.

He was appointed Associate Professor (2001) and Professor (2005) at the Department of Engineering Cybernetics, NTNU. In the academic year 2007–2008, he was a Visiting Professor with The Centre for Complex Dynamic Systems and Control (CDSC), University of Newcastle, Australia. He has

published more than 75 papers at conferences and in journals and is the author of *Compressor Surge and Rotating Stall: Modeling and Control* (London, Springer, 1999), coauthor of *Modeling and Simulation for Automatic Control* (Trondheim, Marine Cybernetics, 2002), and co-editor of *Group Coordination and Cooperative Control* (Berlin, Springer, 2006). His current research interests include mathematical modeling and nonlinear control in general, modeling and control of turbomachinery and control of spacecraft, robots, and nanopositioning devices.

Prof. Gravdahl received the IEEE Transactions on Control Systems Technology Outstanding Paper Award in 2000 and is Member of the Editorial Board of *Simulation Modeling Practice and Theory*.